

CHAPTER 1

INTRODUCTION

1.1 Background of Studies

An Unmanned Aerial Vehicle (UAV) is an unpiloted aircraft which can be controlled from a remote position or flown autonomously based on pre-programmed flight plans or more complex dynamic automation systems. Vertical Take Off and Landing (VTOL) of a UAV refer to the vertical lift off without needing to use a runway or an airstrip. The main focus of the project is to design a mechanism to supplement the quad-rotor fan Micro-UAV which utilizes four fans to provide lift and propulsion for the operation of the Micro-UAV. At rest, the fans will be providing downward thrust which allows for the VTOL capability but the quad-rotor fan design has to be supplemented with another mechanism for forward propulsion of the Micro-UAV. The study will also be about existing VTOL mechanisms as well as other UAVs in developing a stable VTOL mechanism. The project mainly contributes to the automotive cluster which can enhance more understanding in UAV especially for the takeoff and landing mechanism.

1.2 Problem Statement

The vertical take-off and landing function of the quad rotor fan powered Micro Unmanned Aerial Vehicle (MUAV) requires an interlocking mechanism which allows for the vertical and horizontal motion of the MUAV. The mechanism is required to rotate the angle of the fans and lock it in place to perform vertical takeoff and landing operation within MUAV specifications.

1.3 Objectives

To study and design the interlocking mechanism that is capable of the following:

- To rotate the quad rotor to horizontal position
- To lock the engine in the variable angle position

1.4 Scope of Studies

This project focuses on the design of an effective interlocking mechanism that includes the study on its integrity and operation. The project includes:-

- Interlocking mechanism design
- Static analysis
- Dynamic analysis
- Detail drawings and bill of materials

1.5 Relevancy of the Project

This project is relevant to Mechanical Engineering academic syllabus of Universiti Teknologi PETRONAS (UTP). It incorporates knowledge in Mechanical Engineering Design, Manufacturing Technology, Engineering Materials, Dynamics, Statics, Mechanics of Machines, Mechatronics, Vibration, and Computer Aided Engineering Design. This project also provides an opportunity to enhance project management and communication skills.

1.6 Project Feasibility

The first phase of the project is the Problem Definition and Conceptual Design Development. The second phase will be the Embodiment Design Development and Detail Design Development. For FYP1, the project will be concentrated at the first phase. The second phase will be completed in FYP 2. The final output of the project will be the detailed drawings of the design, bill of materials and detailed product specification. Based on the methodology used, the objectives of the project can be achieved within the given time frame.

CHAPTER 2

LITERATURE REVIEW AND THEORY

2.1 UAV Platforms

Unmanned Aerial Vehicles (UAVs) are self-propelled air vehicles that are either remotely controlled or are capable of conducting autonomous operations. UAV experimental research ranges from low-level flight control algorithm design to high level multiple aircraft coordination [1].

During the last decades significant efforts have been devoted to increase the flight endurance and payload of UAVs. Thus, there are High Altitude Long Endurance (HALE) UAVs, as for example the Northrop Grumman Ryan's Global Hawks (65000 ft altitude, 35 h flight and 1900 lbs payload) and Medium Altitude Long Endurance (MALE) UAVs, as for example the General Atomics' Predator (see Figure 2.1, with 27,000 ft altitude, 30/40 h flight and 450 lbs payload), and the Tactical UAVs such as the Pioneer with 15,000 ft altitude, 5–6 h flight and 25 kg payload. In the last years man portable or hand launched UAVs, called "Organics UAV", such as Pointer (AeroVironment), Javelin (BAI) or Black Pack Mini (Mission's Technologies) have been presented.



Figure 2.1: The Predator from General Atomics

Furthermore, many different Vertical Take-Off and Landing (VTOL) UAVs including helicopters and several designs such as the Guardian from Bombardier, and the Sikorsky's Cypher or Dragon Warrior which can be operated in either wings-on (see Figure 2.2) or wings-off configurations [1].



Figure 2.2: The Sikorsky's Dragon Warrior (Cypher2).

On the other hand, in the last years, Micro Air Vehicles with dimensions lower than 15 cm have gained a lot of attention. These include the Black Widow manufactured by AeroVironment (Figure 2.3), the MicroStar from BAE and many new designs and concepts presented in several Universities such as Entomopter (Georgia Institute of Technology), Micro Bat (California Institute of Technology), MFI (Berkeley University), as well as other designs in European Research Centres [1].

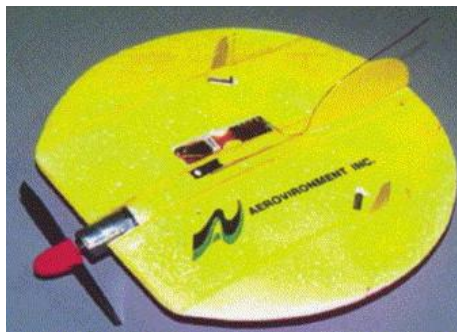


Figure 2.3: Black widow (AeroVironment)

2.2 Harrier Jump Jet (Aircraft with Interlocking VTOL Capability)

To analyze a good VTOL interlocking mechanism design, a study was done on the Harrier Jump Jet. This jet is the world's only vertical takeoff and landing jet fighter. It was developed by the British in an era of financial cutbacks which saw the end of the large Royal Navy Aircraft Carriers. It can use airfields on land or flown from smaller aircraft carriers at sea and is flown by the best US and British pilots. It combines the best aspects of a helicopter with those of a fighter jet. The Harrier's most famous feature is its vertical takeoff and landing capability. Although the Harrier has one jet engine (The Pegasus) it has four nozzles that direct the jet engine thrust downwards

for vertical lift (Figure 2.4). Once airborne the nozzles are slowly revolved so that the plane moves forward (Figure 2.5) [13].

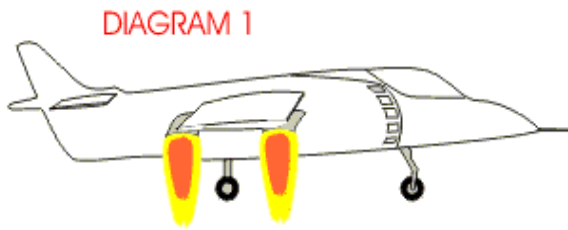


Figure 2.4: Vertical Motion

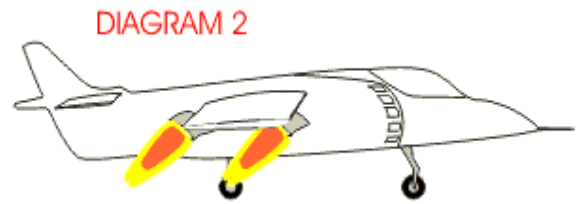


Figure 2.5: Horizontal Motion

The key difference between the Harrier and other combat aircraft is the Pegasus engine. This is a low bypass-ratio turbofan that is similar in operation to other such engines, with the additional feature of four rotating nozzles through which the engine's fan and core airflows exhaust (Figure 2.6). These four nozzles can be rotated through an arc of 98.5 degrees, allowing the engine's thrust to be applied from directly aft (in conventional flight) to straight down (for hovering) to slightly forward (for flying backwards). These nozzle movements are normally actuated using a pneumatic motor operated by engine bleed air. The motor drives a number of shafts and chain drives (Figure 2.7) to ensure that all nozzles operate in unison since difference would lead to a rapid loss of aircraft attitude and control [13].

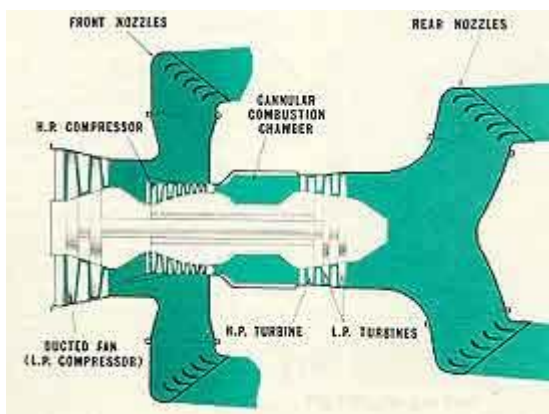


Figure 2.6: Diagram of Pegasus engine airflows, showing the vectoring nozzles.

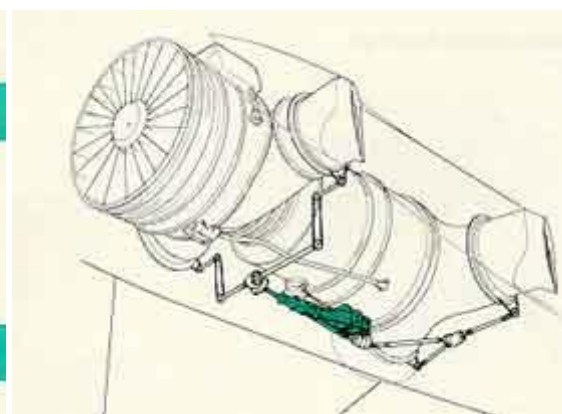


Figure 2.7: Pneumatic motor and nozzle drive system.

2.3 Micro UAV Design

This is the design of Micro UAV based on AutoCAD software that will be utilizing the VTOL mechanism [6]:

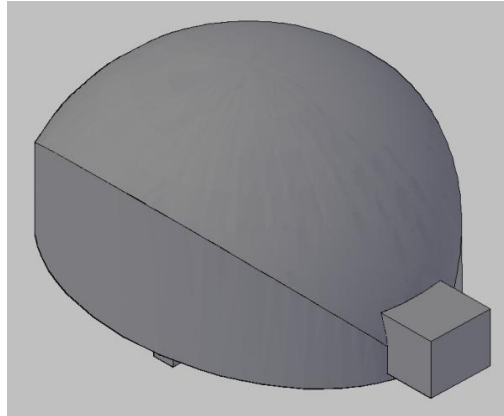


Figure 2.8: 3D view of Micro UAV

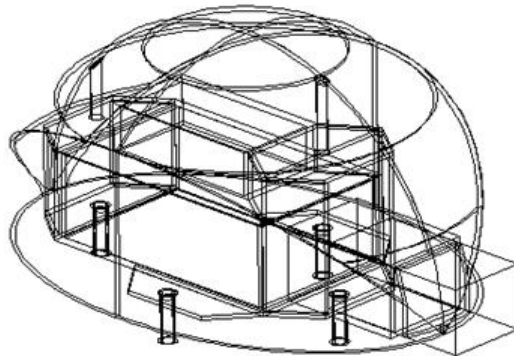


Figure 2.9: NE Isometric View for Micro UAV

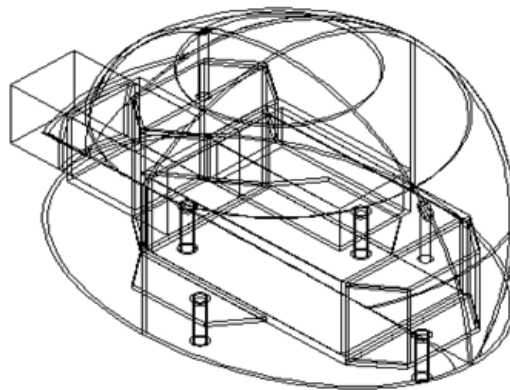


Figure 2.10: SW Isometric View for Micro UAV

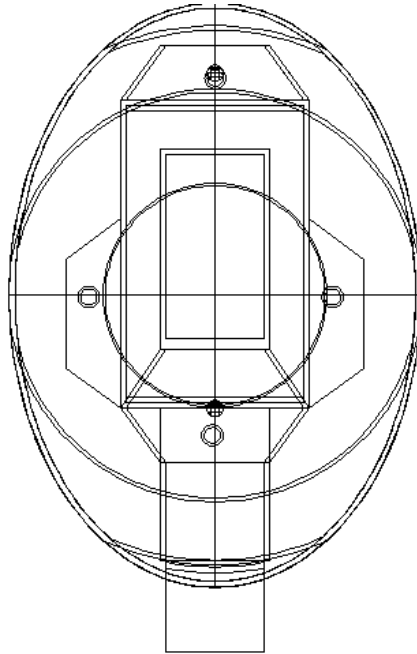


Figure 2.11: Plan View of Micro UAV

2.4 Quad Rotor Fan Design

This is the design of the fan that will be fitted on the mechanism for variable angle position capability [9]:

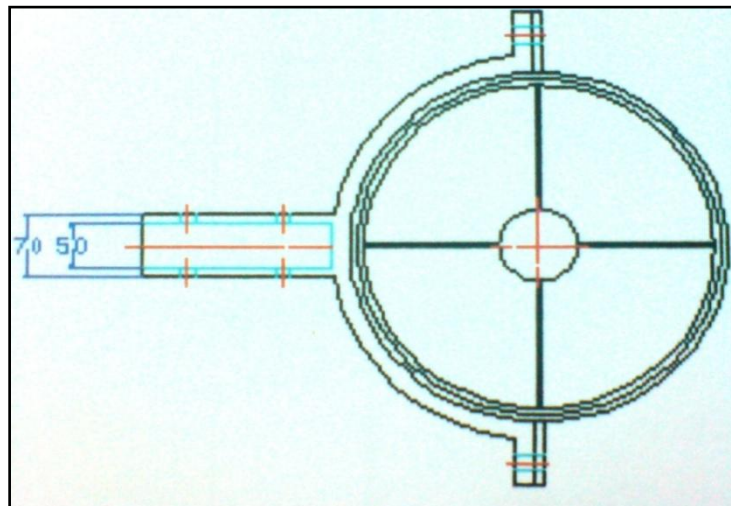


Figure 2.12: Plan View of Fan

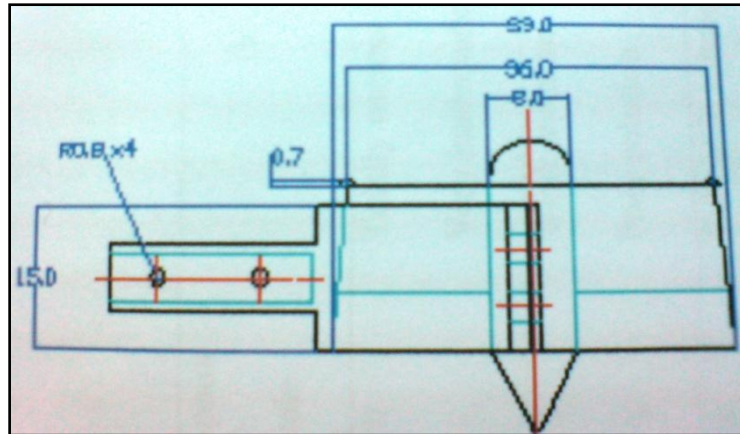


Figure 2.13: Front View of Fan

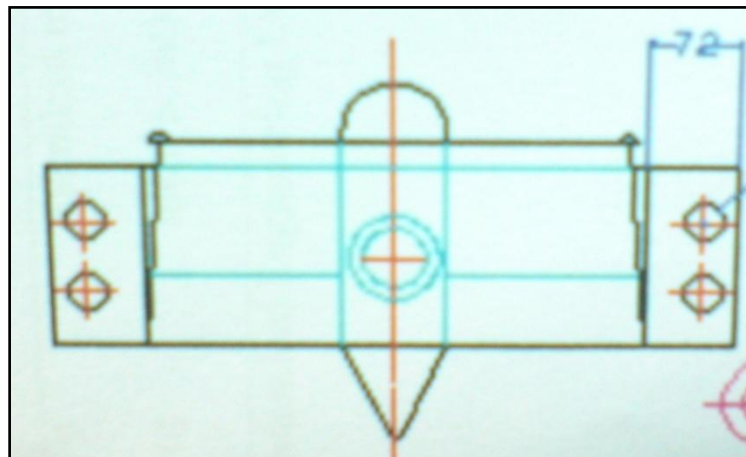


Figure 2.14: Side View of Fan

2.5 Power Transfer Devices

The mechanism will require a power transfer device to efficiently transfer the power from the motor to rotate the fans. A study has been conducted on the possible power transfer devices that can be considered for the design.

2.5.1 Ladder Chain

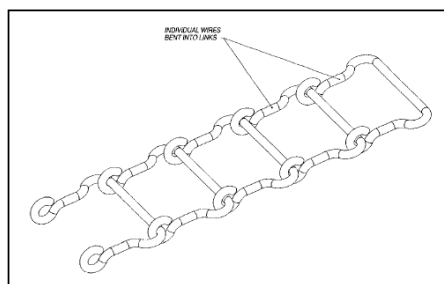


Figure 2.15: Ladder chain

Ladder chain is so named because it looks like a very small ladder. Its construction is extremely simple and inexpensive. A short piece of wire is bent into a U shape and looped over the next U in the chain. Referring to Figure 2.4, this construction is not very strong so this chain is used mainly where low cost is paramount and the power being transferred is less than 1/4 horsepower [2].

2.5.2 Timing Belts

Timing belts solve the slip problems of flat belts by using a flexible tooth, molded to a belt that has tension members built in. The teeth are flexible allowing the load to be spread out over all the teeth in contact with the pulley. Timing belts are part of a larger category of power transmission devices called synchronous drives. These belt or cable-based drives have the distinct advantage of not slipping. Timing belts come in several types, depending on their tooth profile and manufacturing method. The most common timing belt has a trapezoidal shaped tooth. This shape has been the standard for many years, but it does have drawbacks. As each tooth comes in contact with the mating teeth on a pulley, the tooth tends to be deflected by the cantilever force, deforming the belt's teeth so that only the base of the tooth remains in contact. This bending and deformation wastes energy and also can make the teeth ride up pulley's teeth and skip teeth. The deformation also increases wear of the tooth material and causes the timing belt drive to be somewhat noisy. Timing belts can be used at very low rpm, high torque, and at power levels up to 250 horsepower. They are an excellent method of power transfer, but for a slightly higher price than chain or plastic-and-cable chain [2].

2.5.3 Couplers

Couplers are available in two major styles: solid and flexible. Solid couplers must be strong enough to hold the shafts' ends together as if they were one shaft. Flexible couplers allow for misalignment and are used where the two shafts are already running in their own bearings, but might be slightly out of alignment. The only other complication is that the shafts may be different diameters, or have different end details like keyed, hex, square, or smooth. The coupler simply has different ends to

accept the shafts it is coupling. Solid couplers are very simple devices. They clamp onto each shaft tight enough to transmit the torque from one shaft onto the other. The shafts styles in each end of the coupler can be the same or different. For shaped shafts, the coupler need only have the same shape and size as the shaft and bolts or other clamping system to hold the coupler to the shaft. For smooth shafts, the coupler must clamp to the shaft tight enough to transmit the torque through friction with the shaft surface. This requires very high clamping forces, but is a common method because it requires no machining of the shafts [2].

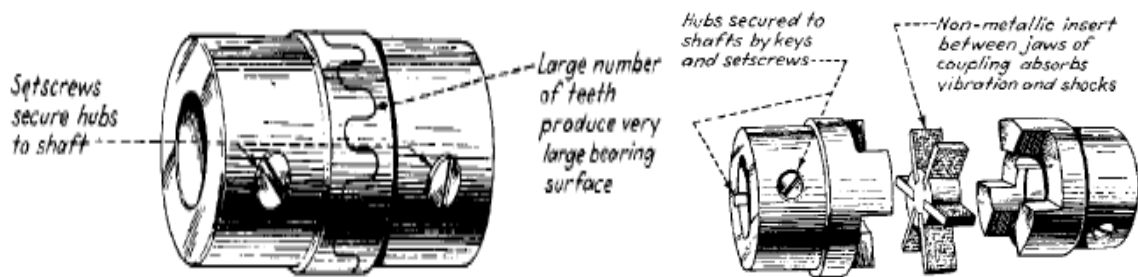


Figure 2.16: Couplers with setscrews

2.6 System Drives

The rotation of the fans will rely on a motor. Thus, a study has been conducted on the possible motors that can best perform the required functions while adhering to the size and design constraints.

2.6.1 Servo Motor

Motors come in many different varieties for different applications. The term servo motor applies to the way in which the motor is used and controlled. In a position servo motor application (henceforth just servo motor.), the idea is to hold the target load (generally attached to the motor shaft through a series of gears for speed and torque adjustment) in a given position [3].

To accomplish a servo motor function, positioning information must be obtained from the output of the motor to provide feedback for the control system. This can be in the form of a potentiometer attached somewhere in the gear train, a hall effect sensor

monitoring passing teeth on a metal gear, an encoder (optical or magnetic) mounted directly to the motor, or any other such sensor which can provide position feedback of the motor shaft or connected portion of the gear train. It is also possible to determine motor shaft position by counting the commutation pulses on the terminals of the motor and measured with an analog-to-digital converter (ADC). In this way, it might be possible to monitor the load current and detect variations in the load current which correspond with the commutation of the brushes in the motor. However, this method requires additional software and hardware complexity which do not justify their inclusion, given that encoders are just as effective and much simpler to implement. This modification allows streamlining of the logic needed at the load to drive it [3].

2.6.2 Stepper Motor



Figure 2.17: Stepper Motor

A stepper or stepping motor is an AC motor whose shaft is indexed through part of a revolution or step angle for each DC pulse sent to it. Trains of pulses provide input current to the motor in increments that can “step” the motor through 360°, and the actual angular rotation of the shaft is directly related to the number of pulses introduced. The position of the load can be determined with reasonable accuracy by counting the pulses entered. The stepper motors suitable for most open-loop motion control applications have wound stator fields (electromagnetic coils) and iron or permanent magnet (PM) rotors. Unlike permanent magnet DC servomotors with mechanical brush-type commutators, stepper motors depend on external controllers to provide the switching pulses for commutation. Stepper motor operation is based on the same electromagnetic principles of attraction and repulsion as other motors, but their commutation provides only the torque required to turn their rotors. Pulses from the external motor controller determine the amplitude and direction of current flow in

the stator's field windings, and they can turn the motor's rotor either clockwise or counterclockwise, stop and start it quickly, and hold it securely at desired positions. Rotational shaft speed depends on the frequency of the pulses. Because controllers can step most motors at audio frequencies, their rotors can turn rapidly. Between the applications of pulses when the rotor is at rest, its armature will not drift from its stationary position because of the stepper motor's inherent holding ability or detent torque. These motors generate very little heat while at rest, making them suitable for many different instrument drive-motor applications in which power is limited [2].

2.6.3 Micro-Drives

Micro-drives are small motors between 6 – 16 mm in diameter. These motors have an extreme small sized design that incorporates high-tech ceramic components. It also uses high energy magnets with optimized volume/performance ratio. The micro-drives come with a complete system which includes motor, gear heads, feedback devices and control electronics [4].

2.6.4 Motor Selection

The vast majority of automated manufacturing systems involve the use of sophisticated motion control systems that, besides mechanical components, incorporate electrical components such as servo motors, amplifiers and controllers. The task for the motion system design is to specify the smallest motor and drive combination that can provide the torque, speed and acceleration as required by the mechanical set up [7].

2.7 Sensors

Sensors are needed to provide inputs for the mechanism to work. The sensors will need to keep track of the shaft position as it rotates to provide the variable angle position function for the mechanism as well as sensors to determine altitude. A study was conducted on sensors that may be applicable for the mechanism.

2.7.1 Rotary Encoders

Rotary encoders, also called rotary shaft encoders or rotary shaft-angle encoders, are electromechanical transducers that convert shaft rotation into output pulses, which can be counted to measure shaft revolutions or shaft angle. They provide rate and positioning information in servo feedback loops. A rotary encoder can sense a number of discrete positions per revolution. The number is called points per revolution and is analogous to the steps per revolution of a stepper motor. The speed of an encoder is in units of counts per second. Rotary encoders can measure the motor-shaft or lead screw angle to report position indirectly, but they can also measure the response of rotating machines directly. The most popular rotary encoders are incremental optical shaft-angle encoders and the absolute optical shaft-angle encoders [2].

2.7.2 Digital Barometric Pressure Sensor

A pressure sensor measures pressure, typically of gases or liquids. It usually acts as a transducer where it generates a signal as a function of the pressure imposed. Pressure sensors can also be used to indirectly measure other variables such as fluid/gas flow, speed, water level, and altitude. Pressure sensors can alternatively be called pressure transducers, pressure transmitters, pressure senders, pressure indicators and piezometers. For altitude sensing, the relationship between changes in pressure relative to the altitude is expressed by the equation below;

$$h = \frac{(1 - (P/P_{ref})^{0.19026}) \times 288.15}{0.00198122} \quad \text{Equation 1}$$

The Bosch BMP085 Digital Pressure Sensor is designed for both altitude and temperature sensing [5].

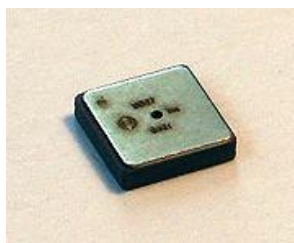


Figure 2.18: Compact Digital Barometric Sensor

CHAPTER 3

METHODOLOGY

3.1 Research

3.1.1 Literary Research

The literary research includes researches made from books, journals and materials from the Internet as mentioned in Literature Review. From these materials, I will be able to better understand the existing systems, methods and theories which will be essential in the development of new ideas in order to develop the interlocking mechanism of the UAV VTOL.

3.1.2 Consultation and Discussion

Obtaining the fundamental theories and reference are done by discussion and consultation with the lecturers. Gathering comments and critics from colleagues will also be a part of the research methodology. The calculations as well as verification of the theory and design will be referred to the supervisor and respective lecturers with expertise in the particular field.

3.2 Tools

The project requires the utilization of several equipment and software. This engineering software will be used in design modeling and analysis.

Table 3.1: Project Tools

Tools	Functions
Autodesk Inventor	Develop CAD model, simulation, design analysis and detailed engineering drawings.
AutoCAD	Develop Sketches
PowerPoint	Develop presentation slides

3.3 Project Activities

The first phase of the project is the Problem Definition and Conceptual Design Development. The second phase will be the Embodiment Design Development and Detail Design Development. For FYP1, the project will be concentrated at the first phase. The second phase will be completed in FYP 2.

The final output of the project will be the detailed drawings of the design, bill of materials and detailed product specification. Figure 3.1 and Figure 3.2 below is the overall flowchart of the entire project and the time allocated for these activities will be illustrated in the Gantt chart in APPENDIX A.

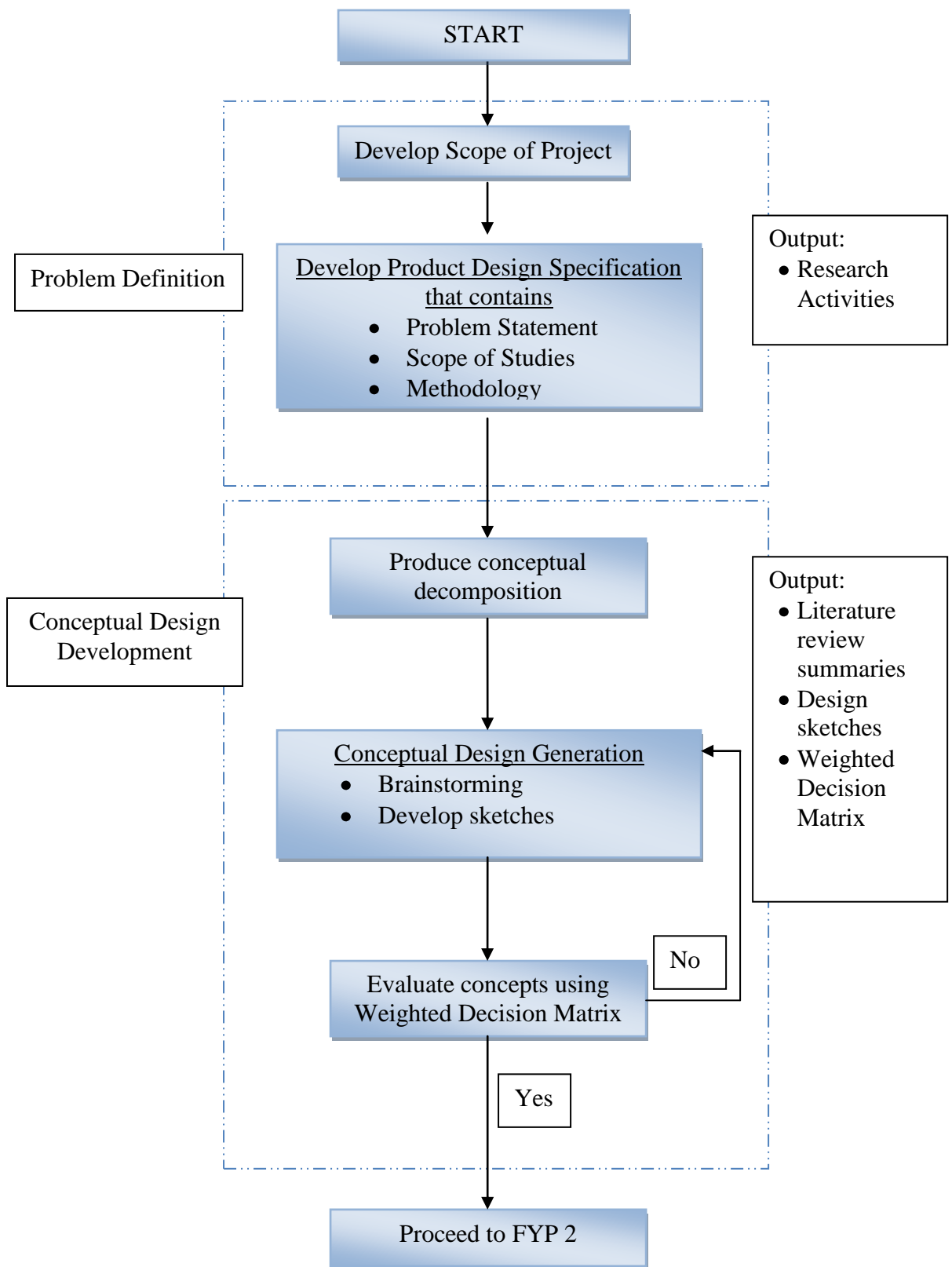


Figure 3.1: Flowchart for FYP 1

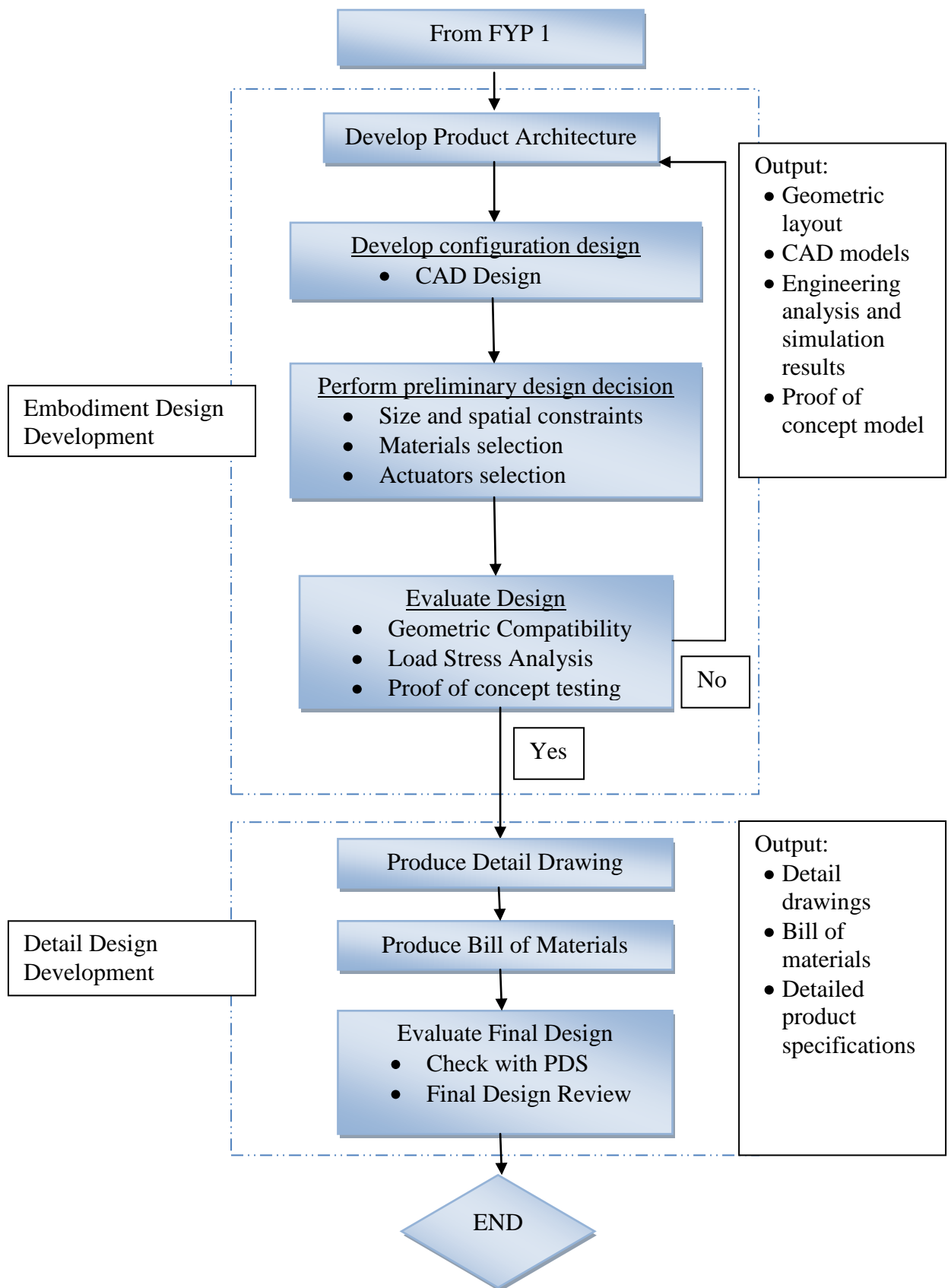


Figure 3.2: Flowchart for FYP 2

3.3.1 Problem Definition

The scope of the project and design specifications will be developed based on the requirements and constraints of the existing Micro-UAV structure and fan design.

3.3.2 Conceptual Design Development

Conceptual decomposition will be done by conducting a literature review on existing MUAVs, drive systems, actuators and power transfer devices. Based on the study, conceptual design alternatives will be generated and evaluated with the Weighted Decision Matrix. Sketches of the design will be done with AutoCAD.

The conceptual design is decomposed into specific components to ease the project design selection and management.

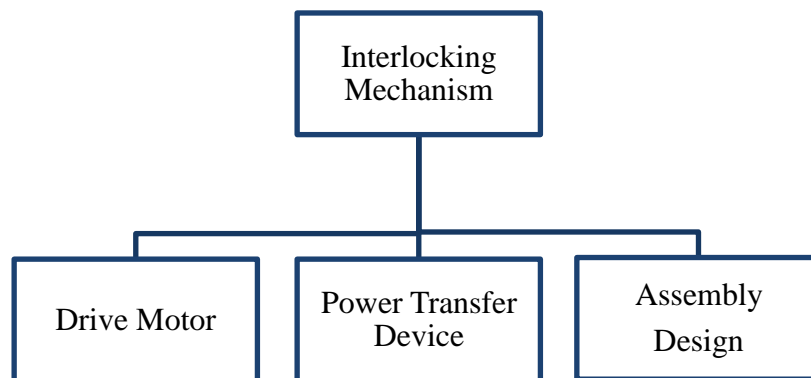


Figure 3.3: Physical decomposition of the mechanism.

3.3.3 Embodiment Design Development

Product architecture and configuration design will be developed and the mechanism will be designed with Autodesk Inventor. Preliminary design decisions will be made followed by design evaluations by conducting stress analysis of the components under static conditions as well as under variable loading conditions.

The shape and general dimensions established in the configuration design is based on the product architecture. Following are the steps taken in the development of configuration design [14]:

- Reviewed the Product Design Specification (PDS).
- Established the spatial constraints
- Created and refined the interfaces or connections between components.
- Eliminated or combined parts and tried to use standard parts to reduce cost.

The output in the configuration design is a CAD model of the interlocking mechanism. The following are also established in the configuration design phase:

- **Size and spatial constraints of each part**

As the design is invested with physical forms, size and spatial constraints are being established with some engineering calculation as the basis. The design evolves according to spatial limitation, part functions and product architecture.

- **Selection of actuators for mechanism**

All mechanisms in the robot design are driven by some sort of actuators. It can be from electromagnetic, pneumatic, or hydraulic types. It is very important to choose the correct type and specification to ensure the design workability and reliability. Proper selection of driving motors is required to ensure the mechanism will be able to operate at the required speed. The following shows the steps used for motor selection:

Purpose: To calculate the torque, motor's angular velocity, total power

Assumptions: Air drag effect is negligible; fan thrust has no effect on torque requirements

Solution:

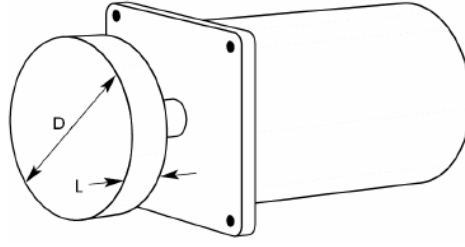


Figure 3.4: Diagram of mechanism concept

To select proper motor, the mechanism is considered to be rotating from one limiting position to another from rest in 0.5 seconds per cycle. Thus from this condition the angular speed and acceleration is obtained using the following equations. [5]

$$\omega = \omega_0 + \alpha_c t \quad \text{Equation 2}$$

$$\theta = \theta_0 + \omega_0 t + \frac{1}{2} \alpha_c t^2 \quad \text{Equation 3}$$

The parameters calculated based on these equations are then used to obtain the total required torque, current and power for motor selection.

Power [8] $P = \tau \omega$ Equation 4

Inertia Calculation [8]

$$J_L = \frac{1}{8} m D^2 = \frac{\pi}{32} \rho L D^4 \quad \text{Equation 5}$$

$$J_T = J_L + J_M \quad \text{Equation 6}$$

Torque Equations [8]

$$T_a = J_T a = (J_L + J_M) \frac{\omega_1 - \omega_0}{t} \quad \text{Equation 7}$$

$$T_T = T_L + T_a \quad \text{Equation 8}$$

$$T_M = K_S T_T$$

Equation 9

J_L – Inertia of the load [kg·m²]

J_M – Inertia of the motor [kg·m²]

J_T – Inertia of the system [kg·m²]

ω_0 – Initial velocity [rad/s]

ω_1 – Final velocity [rad/s]

t – Time for velocity change [s]

T_a – Acceleration torque [N.m]

T_L – Load torque [N.m]

T_T – Total calculation torque [N.m],

T_M – Required motor torque [N.m],

K_S – Safety factor (Reference Value is 1.5 to 2.0.)

- **Selection of Materials**

This is a crucial decision in the design as it links the engineering drawing with a working design. Materials and the manufacturing process which convert the material into a useful part underpin the engineering design.

Autodesk Inventor Professional Stress Analysis will be used to simulate the behavior of the mechanical part under structural loading and dynamic loading conditions. The following material behavior assumptions are applied to this analysis:

- Linear - stress is directly proportional to strain.
- Constant - all properties temperature-independent.
- Homogeneous - properties do not change throughout the volume of the part.
- Isotropic - material properties are identical in all directions.

3.3.4 Detail Design Development

Detail drawings, bill of materials and final design evaluation will be done with Autodesk Inventor.

CHAPTER 4

RESULTS AND DISCUSSION

4.1 Product Design Specifications

The initial specification of the micro UAV is determined as the following:

- Estimated Total Weight of aircraft: 0.2 kg
- Aircraft Dimensions : 5" X 3"
- Total weight of rotating parts: 1 Motor + 1 Rotor + 1 Duct = 39.5 grams

The design specifications of the interlocking mechanism is determined as the following

- Characteristics
 - Lightweight
 - Small and compact
- Capability
 - Lock the engine in the variable angle position
 - Rotate the engine to horizontal position (90 degrees)

4.2 Conceptual Decomposition

The conceptual design is decomposed into several components and analyzed for its suitability to be used for the mechanism design. Table 4.1 shows the possible options that can be used for each component. The pros and cons of each option is considered and then applied to the design concepts.

Table 4.1: Component Options

Components	Options
Drive Motor	<ul style="list-style-type: none"> • Servomotor • Stepper Motor
Power Transfer Device	<ul style="list-style-type: none"> • Ladder Chain • Timing Belt • Couplers • Pulley System
Assembly Design	<ul style="list-style-type: none"> • Motor mounted onto arm joints • Motor mounted within aircraft body

The drive motor can be chosen from servomotors and stepper motors. The advantage of servomotors is that they are faster moving point to point and are better at accelerating very heavy machinery, but at higher maintenance costs. Stepper motors generally are just as accurate as servos and are simpler and more reliable and maintenance free in harsh dusty applications. Both these motors can perform the needed functions, but the size of these motors will be taken into serious consideration due to constraints.

The power transfer devices can be chosen from ladder chains, timing belt, and pulley system which are indirect power transfer devices or the coupler which is a direct power transfer device. The ladder chains are suitable for low-cost and low power applications due to its simple design. The timing belt can be used at very low rpm and high torque but it is more expensive than chains. The pulley system is based on a simple concept at a low cost but it may have an impact on design dimensions. The coupler can transfer power directly between two shafts and it can save space as well as reduce power loss.

The mechanism can either be installed onto the rotating arm joints or inside the aircraft body depending on the power transfer device chosen.

4.3 Design Concepts

4.3.1 Design A

This concept involves rotating the fans with a belt or a chain connected to the drive motor.

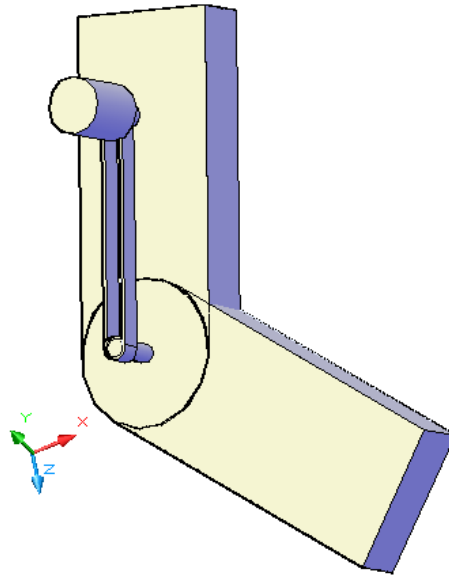


Figure 4.1: CAD sketch of design A.

4.3.2 Design B

The drive motor is connected directly to the joint between the fans and aircraft body with a coupling.

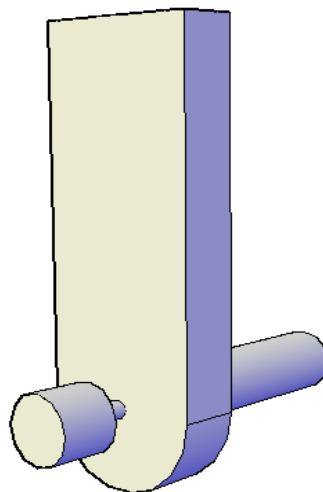


Figure 4.2: CAD sketch of design B.

4.3.3 Design C

The fans are rotated by connecting a wire to the fan and running it through a pulley. The pulley is driven by a motor.

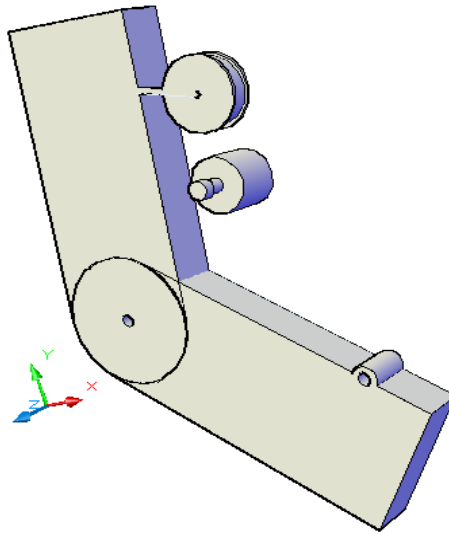


Figure 4.3: CAD sketch of design C.

4.4 Design Concept Evaluation and Selection

From the design concepts generated, all concepts are evaluated and the best concept is picked using the weighted decision matrix based on several criteria. Following are the criteria for evaluation and its weight:

Drive System (0.4)

The drive system is must be power efficient while being able to perform all the necessary functions for the maneuverability of the aircraft. It also has to be simple to reduce maintenance and probability of failure.

- **Functionality (0.6)** – Ability of the system to perform the required functions
- **Simplicity (0.4)** – Simplification of components and assembly to reduce probability of error and little need for maintenance.

Cost (0.1)

The overall cost of the design.

Safety (0.1)

The safety aspects of the design in terms of exposed moving parts as well as potential hazards related to the design of the mechanism.

Physical Shape (0.4)

The shape of the mechanism including the arm, drive motor, power transfer device and the assembly of all components.

- **Size/Dimension (0.5)** – A small design is required for this mechanism.
- **Weight (0.5)** – Lighter design requires less power consumption.

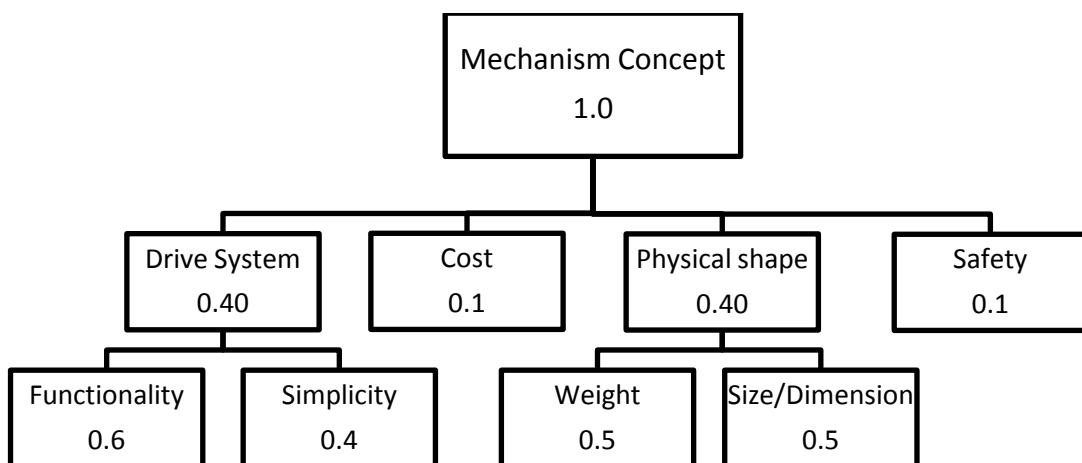


Figure 4.4: Ratings for decision matrix

Table 4.2: Weighted decision matrix for Micro-UAV VTOL mechanism

Design criterion	Weight Factor	Design A		Design B		Design C	
		Score	Rating	Score	Rating	Score	Rating
Functionality	0.24	2	0.48	3	0.72	1	0.24
Simplicity	0.16	1	0.16	2	0.32	3	0.48
Weight	0.20	2	0.40	3	0.60	1	0.10
Size/Dimension	0.20	2	0.40	3	0.60	1	0.10
Cost	0.10	1	0.10	3	0.30	2	0.20
Safety	0.10	2	0.20	3	0.30	1	0.10
		1.74		2.84		1.22	

Design B is chosen based on the weighted decision matrix with a highest score of 2.84.

4.5 Mechanism Working Principle

The mechanism will be designed in two parts which is the arm and driveshaft driven with a selected motor. The arm is connected to the aircraft and acts as the support structure for the mechanism where it will hold the combined weight of the whole mechanism and fan. The operation of this mechanism is based on the torque applied by the motor to the driveshaft whereby the fan will be connected to the end of this driveshaft to allow for variable angle position of the fans. Input to the motor is dependent on the control system of the aircraft and the motor will consume power from the aircrafts battery pack.

4.6 Product Architecture

The product architecture as shown in Figure 4.5 is developed from the selected design. It shows the arrangement of the physical elements of the robot to carry out the required functions.

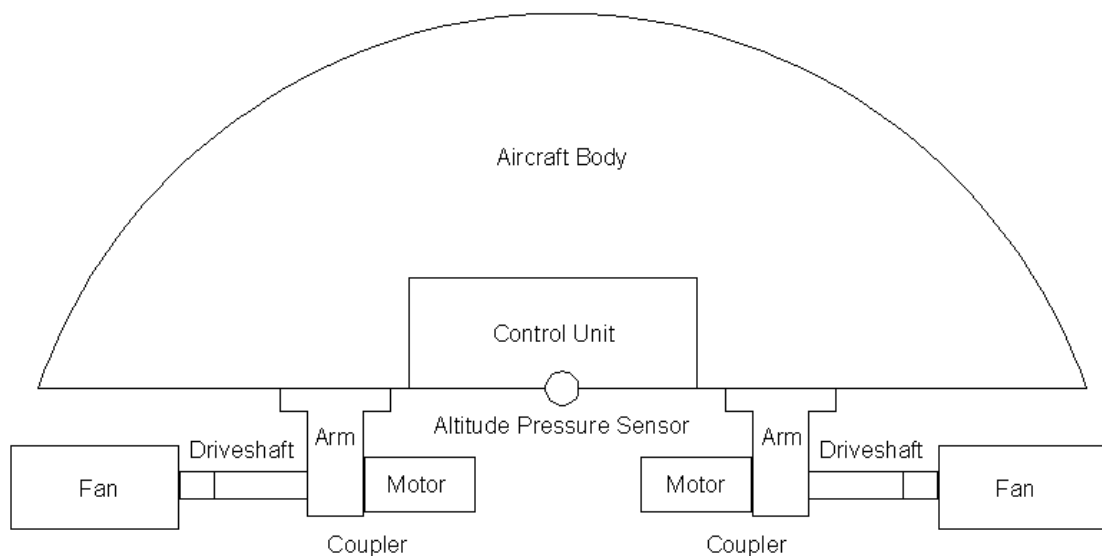


Figure 4.5: Geometric layout of the Micro-UAV

The control board is an important part of the Micro-UAV. It gives and receives signal to all actuators and sensors for it to perform its designed functions. The control system is an integral part of the MUAV and it is vital in the development of the

prototype. However it will not be designed in detail since it is outside of the project scope.

The MUAV receives input from two (2) sensors which are the encoder and digital pressure sensor. The encoder is used to sense the rotation of the fans for it to be in a variable angle position. The digital pressure sensor is used to determine altitude and temperature. This ability to determine altitude may be useful for future development of the MUAV especially if it is designed to be fully automated instead of remotely controlled. In the scope of mechanical design, the mechanism can be divided into three parts which is the motor selection, arm design, and coupler design.

4.7 Development of Configuration Design

4.7.1 Actuator Selection

A simple DC motor with encoder will be used to drive the mechanism. This is due to its simplicity and availability. Based on the analysis made, the required motor specification has been obtained as shown in Table 4.3 below.

Table 4.3: Summary of Motor Specification Analysis

INPUT		
Total mass of rotating parts, m	43.2×10^{-3}	kg
Diameter of link, D	0.005	m
Maximum angle of rotation	90	deg
Desired cycle time, t	0.5	sec
Safety factor	1.5	

OUTPUT		
Angular velocity, ω	6.2832	rad/s
	60	rpm
Minimum Required Torque, T_{min}	3.1094	mNm
Minimum Required Power, P_{min}	0.020	W
Required Torque, T	9.3347	mNm
Required Power, P	0.059	W

While any motor that satisfies these specifications as well as the spatial constraints can be used, the following motor is chosen as a possible option for the driving mechanism.

Precision MicroDrivers 12mm Inline Gear Motor (Double Ended Type)

Model 212-409



Figure 4.6: Precision Microdrivers 212-409

Volts	: 12 V	Speed Range	: 60 – 78 rpm
Diameter	: 12 mm	Torque	: 0.059 Nm
Length	: 24 mm	Power	: 576 mW
Shaft Diameter	: 3 mm	Current	: 119 mA
Weight	: 9.4 g	Gear Ratio	: 298

4.7.2 Material Selection

The mechanism must be made of a light weight rigid material to satisfy the design requirements of the mechanism. There are two possible materials that can be used for the mechanism which are:

1. Aluminum 6061
2. Carbon-Carbon composites

Table 4.4: Properties of Aluminum 6061

Physical Properties	Metric
Density	2.7 g/cm ³
Mechanical Properties	
Hardness, Brinell	30
Ultimate Tensile Strength	124 MPa
Tensile Yield Strength	55.2 MPa
Modulus of Elasticity	68.9 GPa
Poisson's Ratio	0.33
Fatigue Strength	62.1 MPa
Machinability	30%
Shear Modulus	26 GPa
Shear Strength	82.7 GPa
Thermal Properties	
Heat Capacity	0.896 J/g- °C
Thermal Conductivity	180 W/m-K
Melting Point	582-652 °C

Aluminum is a common material in aerospace and robotics. It is very strong, light, resistant to corrosion, and affordable. Most importantly, it is very easy to cut, shape, drill, and bend. Aluminum is not as strong as steel, and rarely as cheap. However, aluminum has a much higher strength to weight ratio which means that for a mass of aluminum and an equal mass of steel, aluminum would be much stronger.

Table 4.5: Carbon-Carbon Composites [17]

Physical Properties	Metric
Density	1.8 g/cm ³
Mechanical Properties	
Ultimate Tensile Strength	275 MPa
Modulus of Elasticity	200 GPa
Poisson's Ratio	0.05
Shear Modulus	24.2 GPa
Shear Strength	191 GPa
Thermal Properties	
Thermal Conductivity	101 W/m-K
Melting Point	3000 °C

The most important class of properties of carbon-carbon composites is their thermal properties. C-C composites have very low thermal expansion coefficients, making them dimensionally stable at a wide range of temperatures and they have high thermal conductivity. Other properties of the carbon-carbon composites include low-weight, high abrasion resistance, high electrical conductivity, non-brittle failure, and resistance to biological rejection and chemical corrosion. Carbon-carbon composites are very workable, and can be formed into complex shapes. [17]

4.8 Mechanism Design

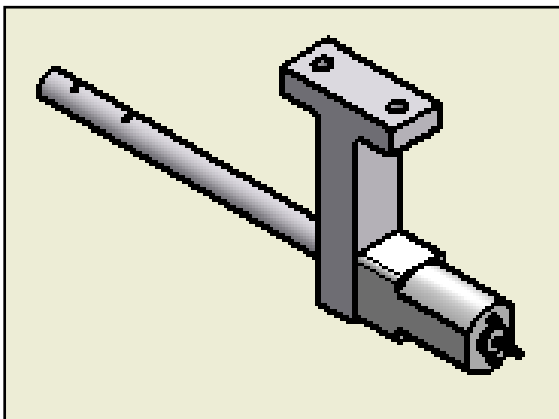


Figure 4.7: Mechanism top right view

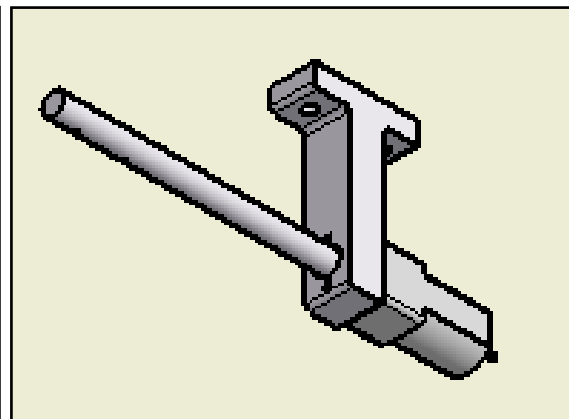


Figure 4.8: Mechanism bottom left view

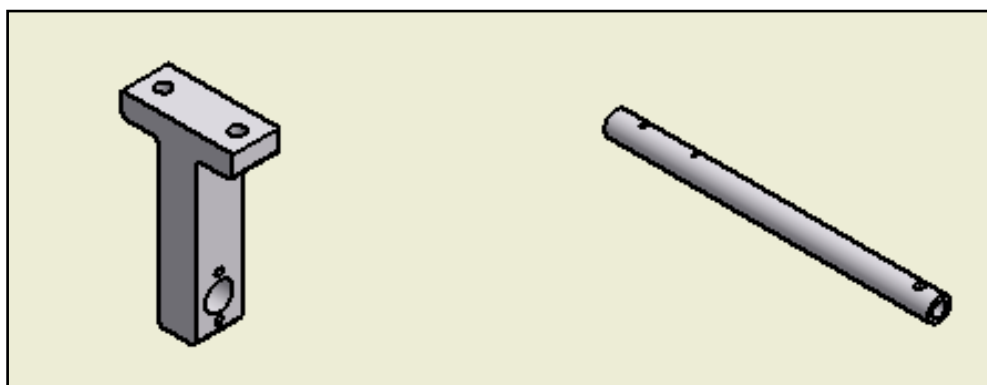


Figure 4.9: Top left view of structure (left) and driveshaft (right)

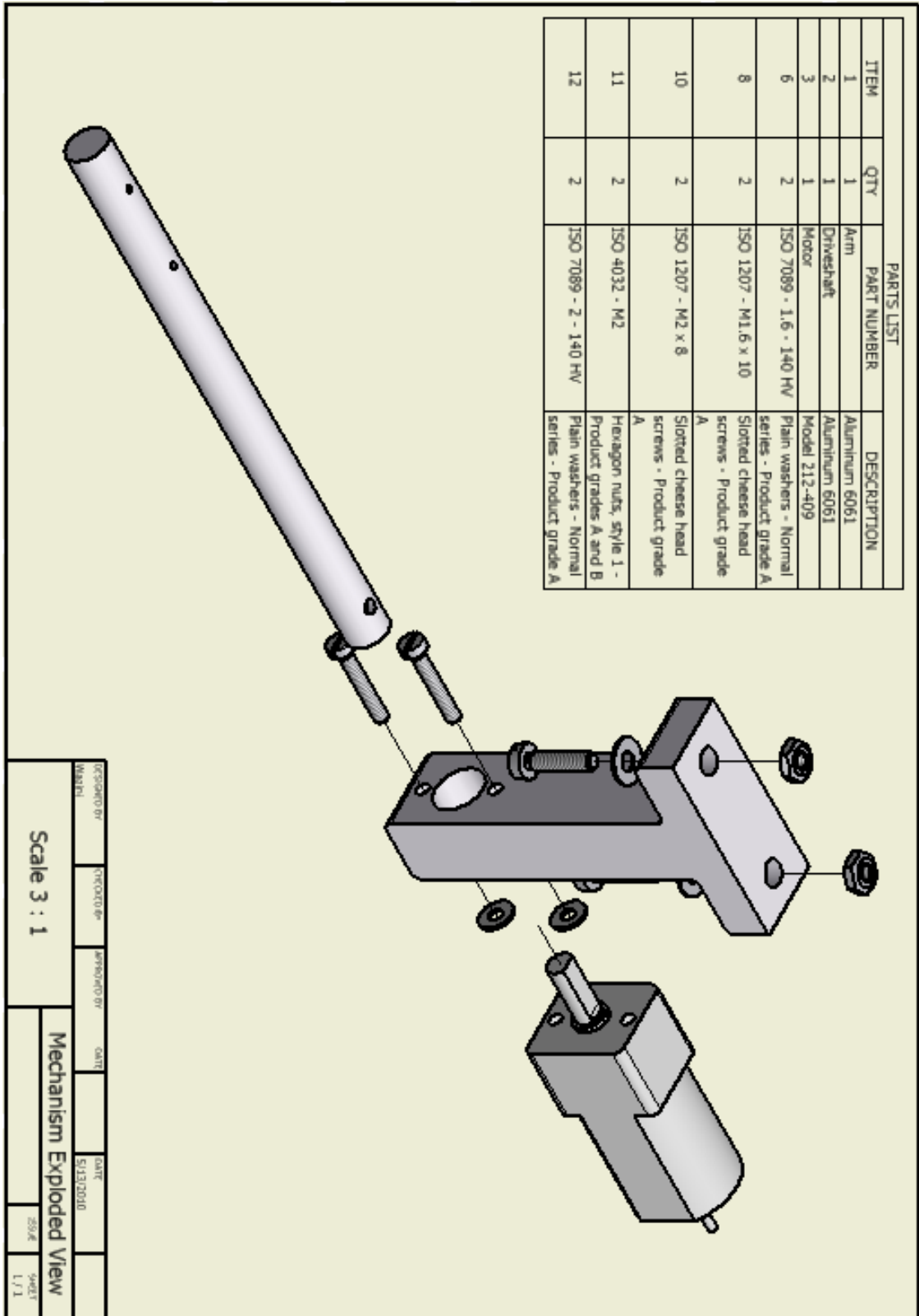


Figure 4.10: Exploded View of Mechanism

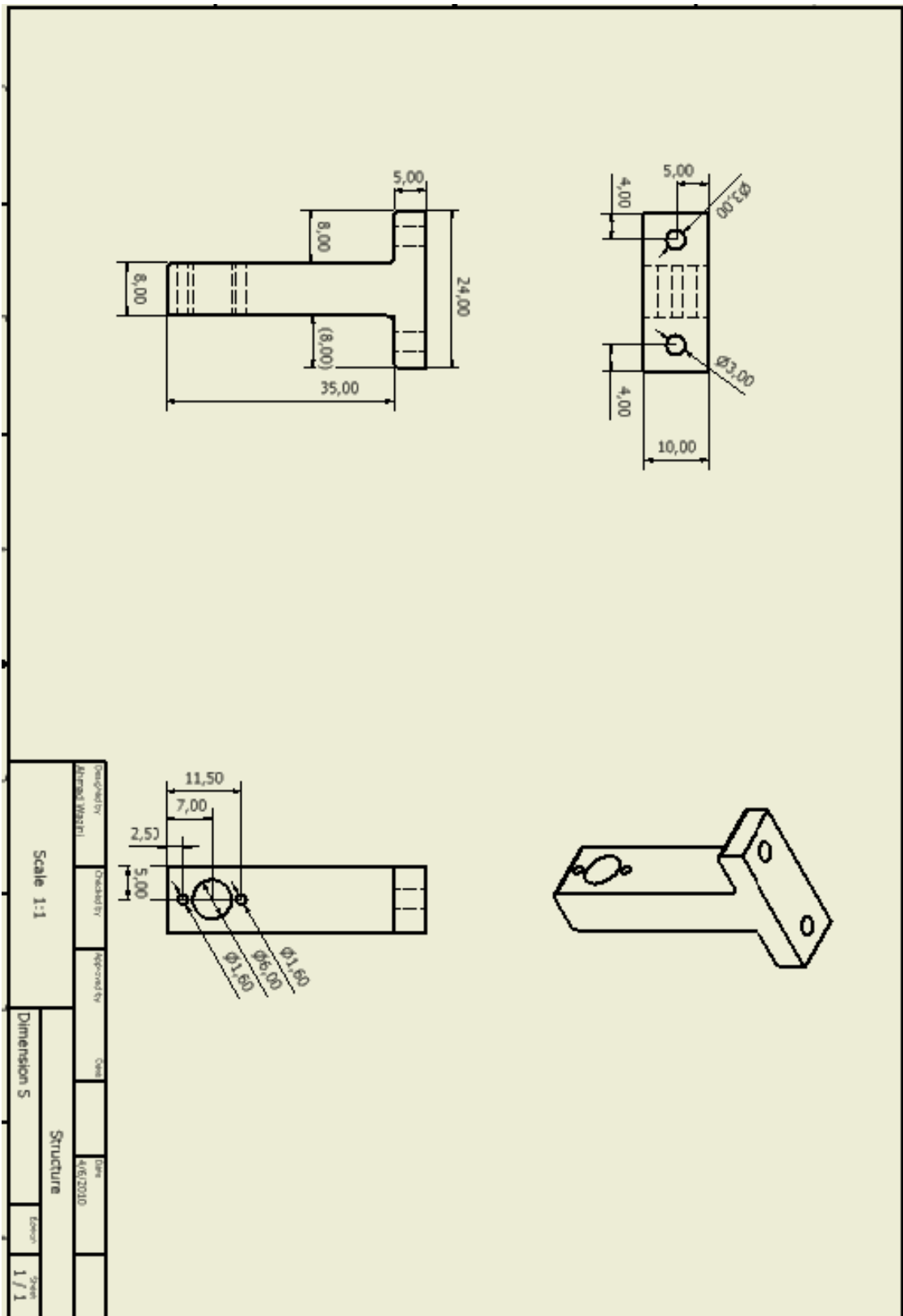


Figure 4.11: Arm with dimension

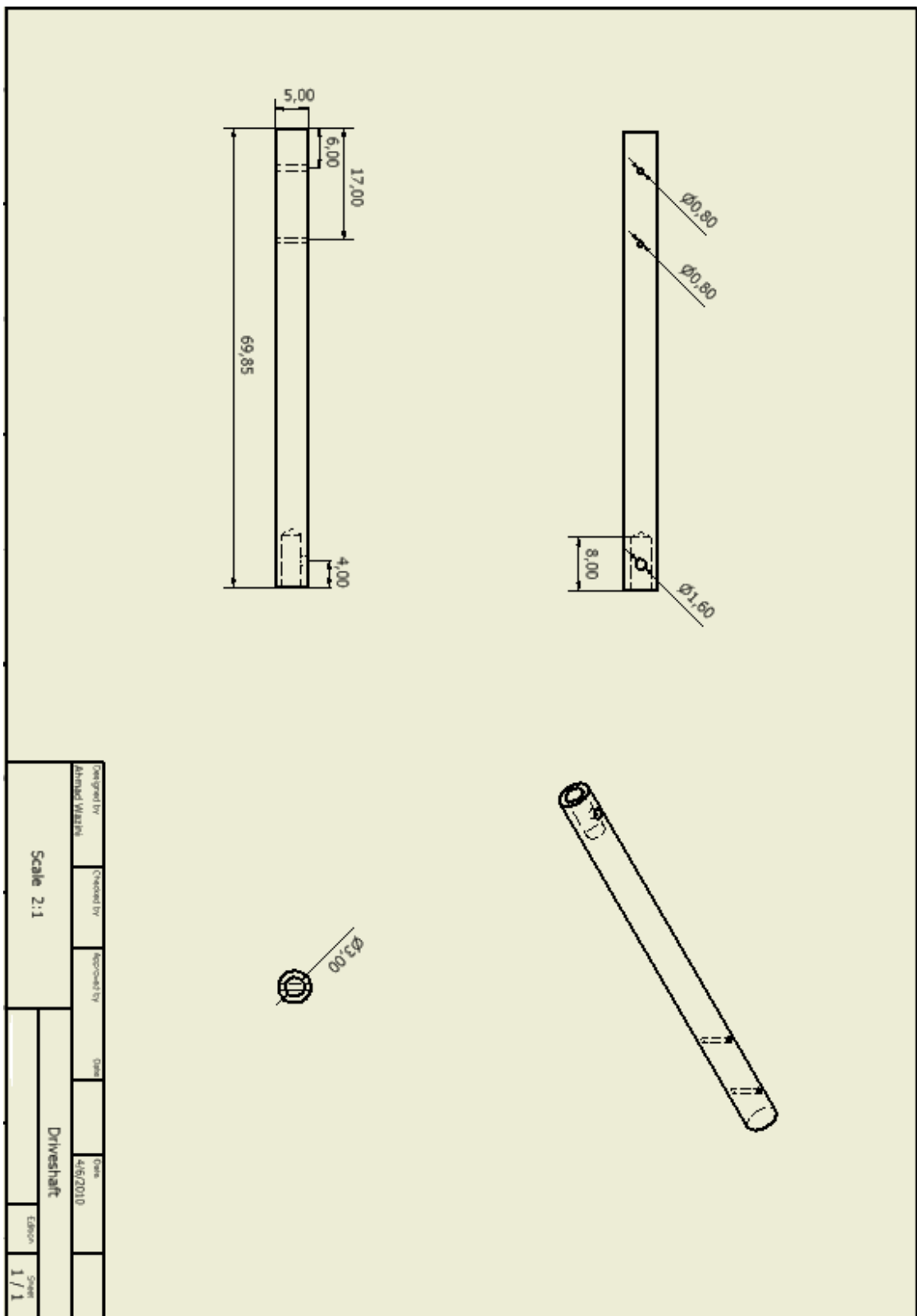


Figure 4.12: Driveshaft with dimension

4.9 Design Analysis

The Relevance setting controls the fineness of the mesh used in this analysis. For reference, a setting of -100 produces a coarse mesh, fast solutions and results that may include significant uncertainty. A setting of +100 generates a fine mesh, longer solution times and the least uncertainty in results. These settings will be shown in the statistics table.

Table 4.6: Arm Statistics

Bounding Box Dimensions	X: 24.0 mm Y: 40.0 mm Z: 10.0 mm
Part Mass	9.937e-003 kg
Part Volume	3667 mm ³
Mesh Relevance Setting	100
Nodes	8100
Elements	4360

Table 4.7: Driveshaft Statistics

Bounding Box Dimensions	5.0 mm 5.002 mm 69.85 mm
Part Mass	3.539e-003 kg
Part Volume	1306 mm ³
Mesh Relevance Setting	100
Nodes	6063
Elements	3355

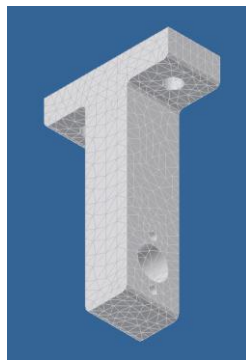


Figure 4.13: Arm Meshing



Figure 4.14: Driveshaft Meshing

4.9.1 Static Analysis of Arm

The arm serves as the link between the rotating parts and the MUAV body. At static conditions it supports the total weight of all the parts while providing a platform for the attachment of the mechanism motor. Below are the boundary conditions;

Table 4.8: Boundary Conditions for Arm Static Analysis

Boundary Condition	Direction	Magnitude
Moment of load	Z-Axis	29.75 N mm
Weight of load	-Y-Axis	0.426 N

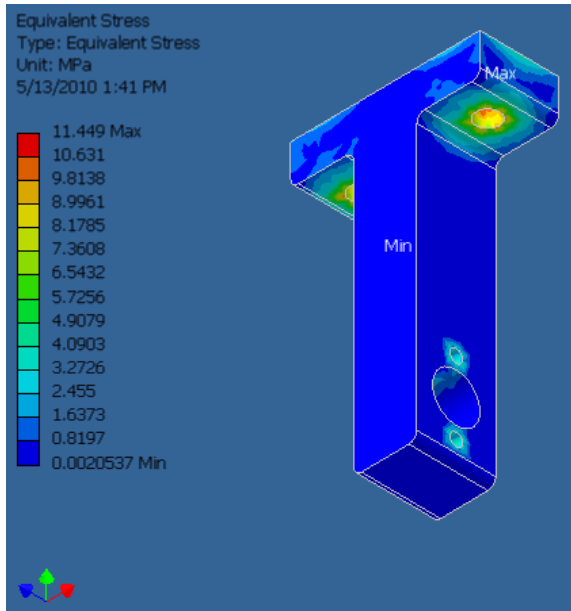


Figure 4.15: Arm Equivalent Stress (MPa)

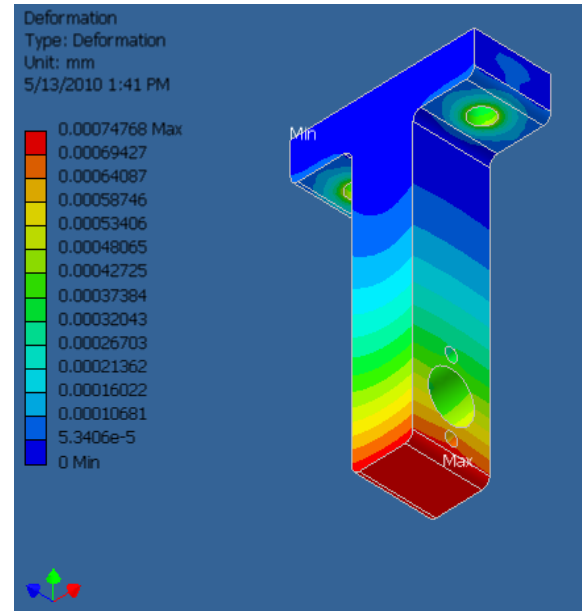


Figure 4.16: Arm Deformation (mm)

Figure 4.15 shows the stress distribution on the structure at static conditions with a maximum magnitude of 11.45MPa where it is mostly concentrated on the holes specifically at the top where the whole mechanism is fastened to the MUAV body. Figure 4.16 shows that the deformation is most significant at the bottom of the arm at 0.00075mm. Deformation at this point is expected due to the fact that the arm experiences bending moment due to the weight of the load acting downwards through the distance of the shaft. These areas should be considered as a critical area in a worst case scenario along with the other holes on the arm that acts as a stress concentration area. Based on these figures the stresses related are well below the yield strength which indicates that the mechanism has a potential to withstand greater loads. The deformation is also extremely low and at these values it does not pose any significant changes in the dimensions of the arm.

4.9.2 Static Analysis of Driveshaft

The shaft serves as the component that transfers the rotational motion from the motor to the fans. At static condition it holds the weight of the fans. Below are the boundary conditions;

Table 4.9: Boundary Conditions of Driveshaft Static Analysis

Boundary Condition	Direction	Magnitude
Holding force for 1.6mm diameter cup-point socket setscrew ^[16]	Z-Axis	110.00 N
Weight of fan	-Y-Axis	0.40 N

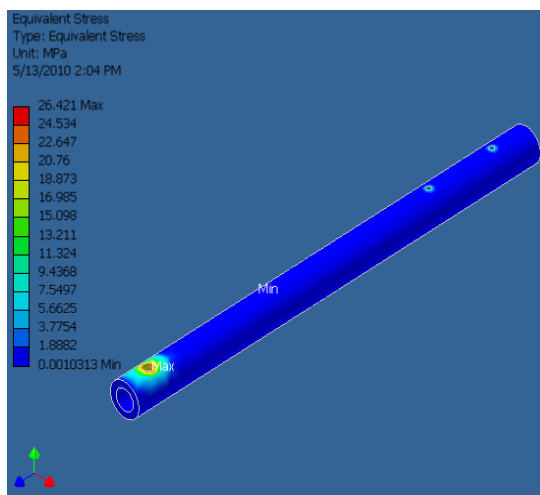


Figure 4.17: Driveshaft Equivalent Stress (MPa)

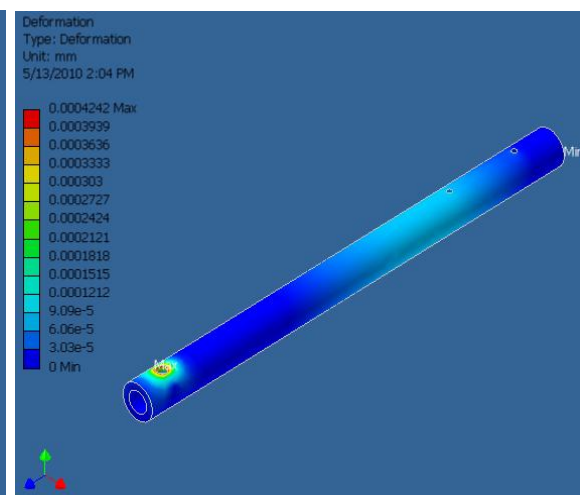


Figure 4.18: Driveshaft Deformation (mm)

Figure 4.17 shows the stress distributions across the driveshaft where the maximum stress of 26.42MPa occurs close to the end where the shaft is coupled to the motor shaft at the setscrew hole. The stress involved is mostly due to the fasteners and setscrew as well as the bending moment experienced due to the weight of the fans on one end. The stress distribution is unclear due to the substantial difference between the high holding power of the setscrew and the low average stress across the shaft. Figure 4.18 shows the deformation of the shaft where the greatest deformation occurs at the setscrew hole at 0.0004mm. Based on these results, these points can be considered as critical points in a worst case scenario. However, the stresses related are well below the yield strength which indicates that the mechanism has a potential to

withstand greater loads. The deformation is also extremely low and at these values it does not pose any significant changes in the dimensions of the arm.

4.9.3 Dynamic Analysis of Arm

The analysis of the arm under variable loading is conducted to investigate the effects of these changing loads on the stress and deformation concentrations on the arm. The variable boundary condition for this analysis is the moment created by the thrust of the fan which is transferred to the arm through the shaft. Below are the values of this varied boundary condition.

Table 4.10: Boundary Conditions for Arm Dynamic Analysis

Moment due to fan thrust	Direction	Magnitude
Hovering Condition	Z-Axis	140.00 N mm
Full Operating Condition	Z-Axis	350.00 N mm
Extreme Condition	Z-Axis </td <td>1000.00 N mm</td>	1000.00 N mm

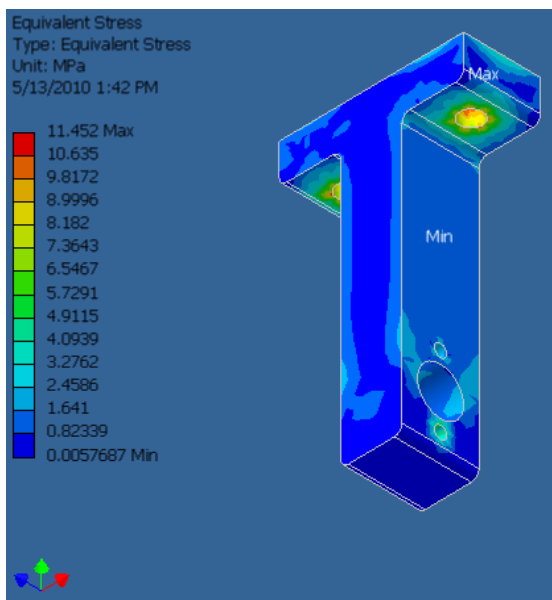


Figure 4.19: Arm Equivalent Stress at hovering condition (MPa)

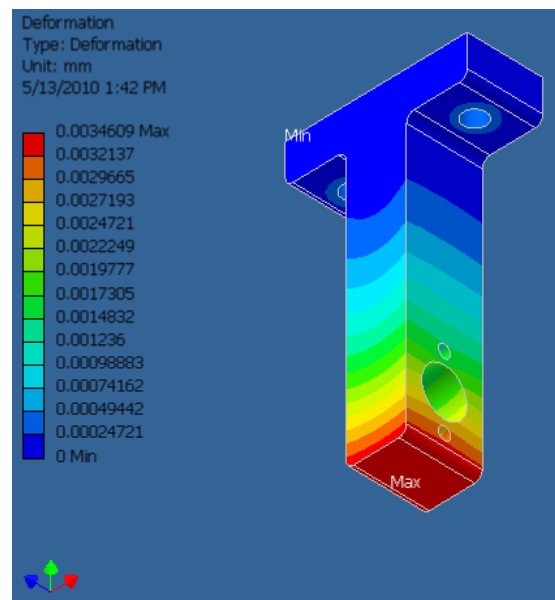


Figure 4.20: Arm Deformation at hovering condition (mm)

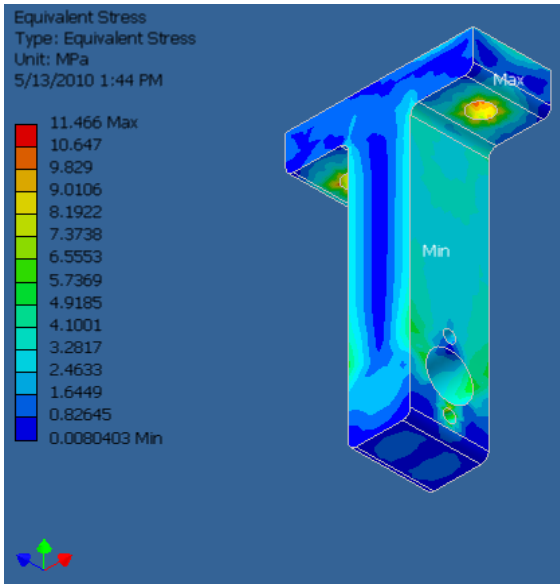


Figure 4.21: Arm Equivalent Stress at full operating condition (MPa)

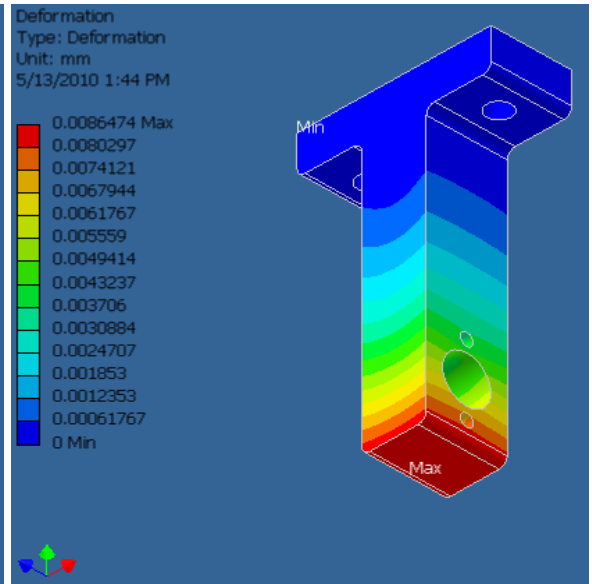


Figure 4.22: Arm Deformation at full operating condition (mm)

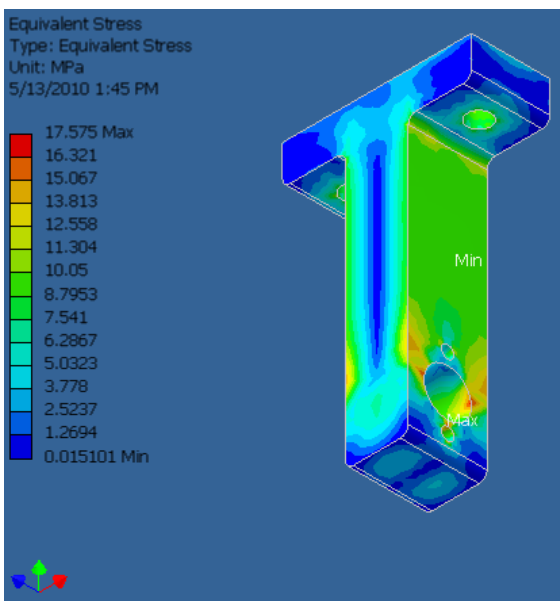


Figure 4.23: Arm Equivalent Stress at extreme condition (MPa)

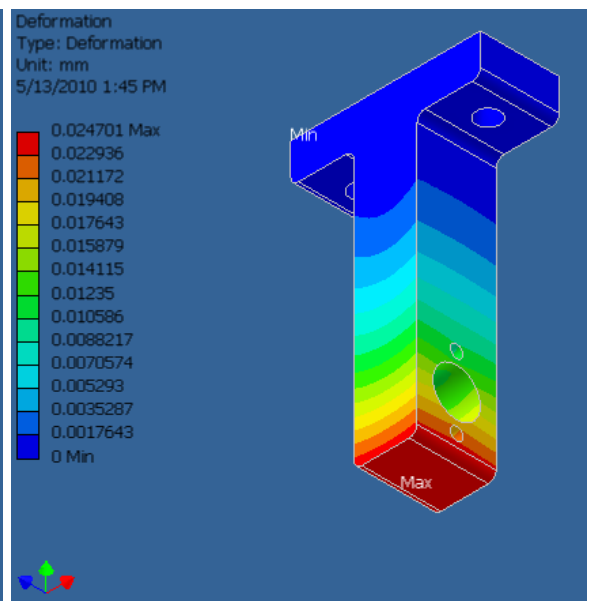


Figure 4.24: Arm Deformation at extreme condition (mm)

Table 4.11: Summary of Arm Dynamic Analysis Results

Operating Condition	Maximum Equivalent Stress (MPa)	Maximum Deformation (mm)
Hovering	11.45	0.003
Full Thrust	11.46	0.009
Extreme	17.58	0.025

Figure 4.19 and Figure 4.20 shows the respective stress and deformation distributions of the arm at hovering mode where the fans generate enough thrust to counter the weight of the MUAV. The arm experiences moment from the thrust of the fan through the driveshaft which results in the stress concentrations at and around the holes. The deformation is most significant at the bottom of the arm.

Figure 4.21 and Figure 4.22 shows the respective stress and deformation distributions of the arm at full operating condition where the fans are at full speed and generating full thrust. The moment resulting from this thrust exerts stress on the arm at and around the holes especially at the shaft and motor holes. The maximum stress still seems to be at the top fastened end of the arm while the deformation is most significant at the bottom of the arm.

Figure 4.23 and Figure 4.24 shows the respective stress and deformation distributions of the arm at extreme conditions where the fans are simulated to have more than twice its designed thrust. The moment resulting from this thrust exerts stress on the arm at and around the holes most significantly at the shaft and motor holes which is greater than the stress due to the force by the fasteners at the top holes. The deformation is most significant at the bottom of the arm.

Based on these results, the stress and deformation seems to be concentrated at similar points on the arm. These points are consistent with the points highlighted as the possible critical areas in the static analysis. Although the stress and deformation occur at similar points, the results show that the magnitude of these stresses and deformations increase proportionally with respect to the thrust generated by the fan. However, these stress values are still below the yield strength of the material which suggests that the design can well withstand the stresses involved in the normal operating conditions and the deformation of the arm is at a low level such that at these values it does not result in any significant changes in the dimensions of the arm.

4.9.4 Dynamic Analysis of Driveshaft

The analysis of the shaft under variable loading is conducted to investigate the effects of these changing loads on the stress and deformation concentrations on the shaft. The

torque applied by the motor to the shaft is varied while maintaining the fan speed and thrust at maximum designed operating capacity. Below are the values of the varied boundary condition.

Table 4.12: Boundary Conditions for Driveshaft Dynamic Analysis

Motor Torque	Direction	Magnitude
Holding Torque (Angle Lock)	Z-Axis	3.11 N mm
Full Torque (Variable Angle)	Z-Axis	9.33 N mm
Maximum Motor Torque	Z-Axis	59.00 N mm

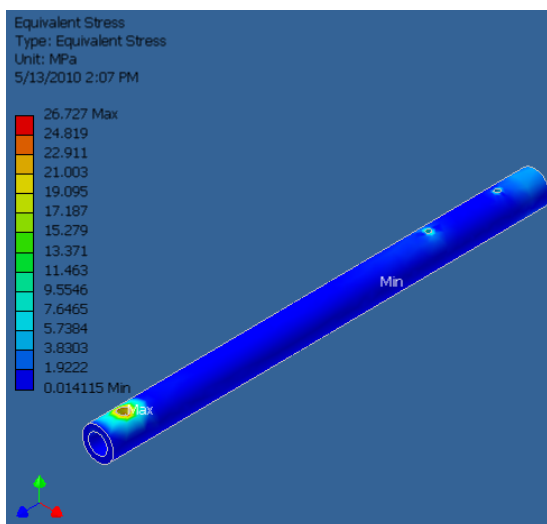


Figure 4.25: Driveshaft Equivalent Stress at holding torque (MPa)

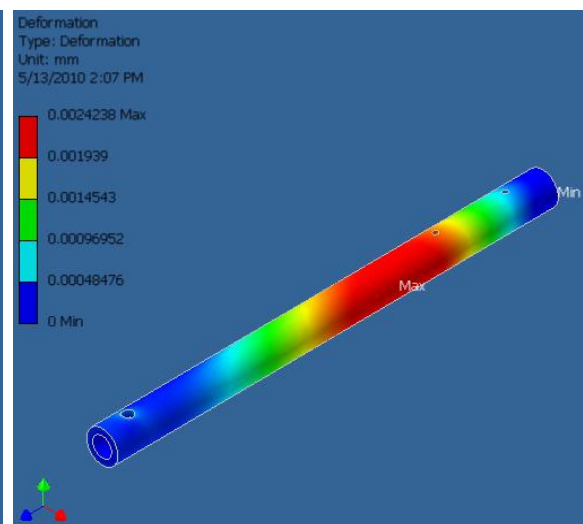


Figure 4.26: Driveshaft Deformation at holding torque (mm)

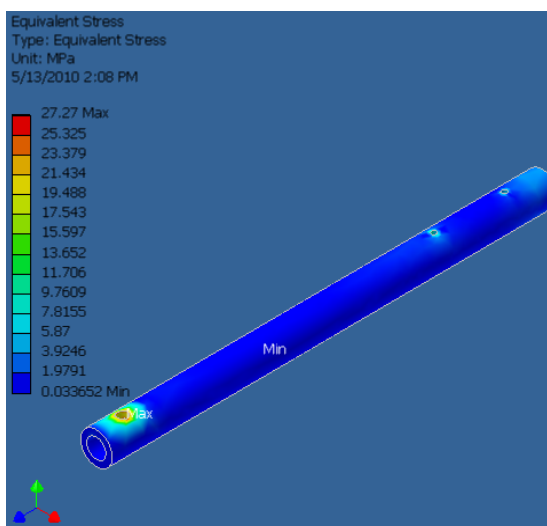


Figure 4.27: Driveshaft Equivalent Stress at full torque (MPa)

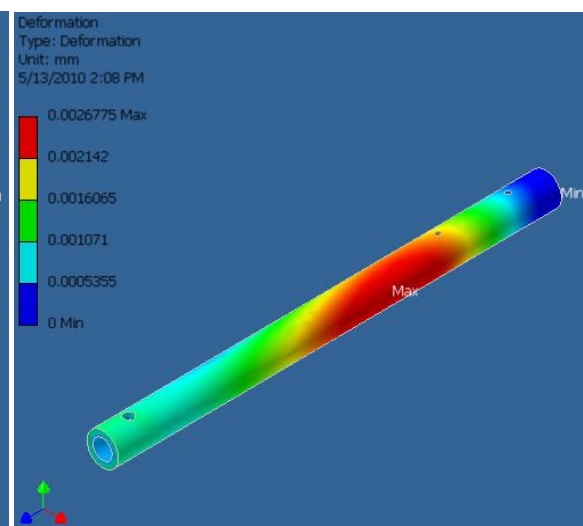


Figure 4.28: Driveshaft Deformation at full torque (mm)

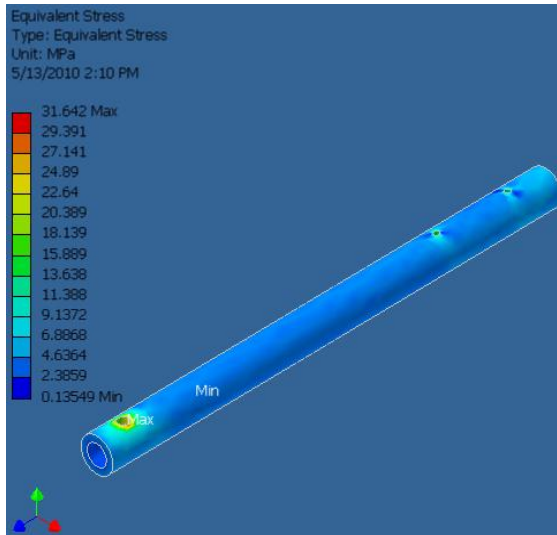


Figure 4.29: Driveshaft Equivalent Stress at maximum motor torque (MPa)

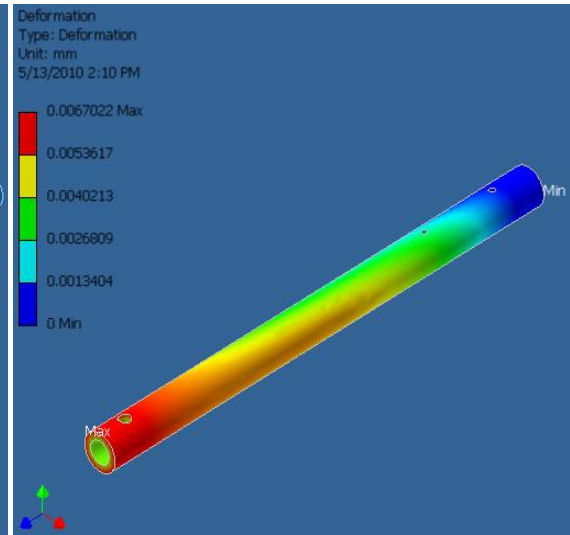


Figure 4.30: Driveshaft Deformation at maximum motor torque (mm)

Figure 4.25 and Figure 4.26 shows the respective stress and deformation distributions of the shaft at holding torque where the fan is locked in position by a constantly applied torque on the shaft. This torque along with the holding force of the setscrew at the motor end of the shaft results in the stress concentration in that area. Stress at the fan end of the shaft specifically at the holes is also visible due to the bending moment and force caused by the thrust of the fan. The deformation of the shaft in this condition is shown to be concentrated at the middle of the shaft due to the bending force mentioned earlier.

Figure 4.27 and Figure 4.28 shows the respective stress and deformation distributions of the shaft at full torque where the shaft is rotated for variable angle control of the fan. This torque along with the holding force of the setscrew at the motor end of the shaft results in the stress concentration in that area. Stress at the fan end of the shaft specifically at the holes is also visible due to the bending moment and force caused by the thrust of the fan. The deformation of the shaft in this condition is shown to be concentrated at the middle of the shaft due to the bending force. However, compared to the previous operating condition, the deformation is shown to be even more significant in towards the motor end of the shaft due to the greater torque being applied.

Figure 4.29 and Figure 4.30 shows the respective stress and deformation distributions of the shaft at maximum torque where the shaft is rotated at highest possible motor torque for variable angle control of the fan. The stress distribution along the shaft is even more visible due to the applied torque with the hole at the motor end again showing the greatest concentration of stress at with a higher magnitude than the previous conditions. The deformation of the shaft in this condition is shown to be concentrated at the motor end of the shaft due to the much higher applied torque.

Based on these results, the stress seems to be concentrated at similar points on the arm. These points are consistent with the points highlighted as the possible critical areas in the static analysis. Although the stresses occur at similar points, the results show that the magnitude of these stresses increase with respect to the increasing torque applied by the motor to the shaft. However, these stress values are is still below the yield strength of the material which suggests that the design can well withstand the stresses involved in the normal operating conditions.

The deformation of the shaft is shown to shift towards the motor end of the shaft as the torque increases. Due to this it can be summarized that the bending stress due to the fan thrust contributes to the most deformation on the shaft at lower shaft torque while at higher torques, the motor end of the shaft may be experience greater deformation. However, the deformation of the shaft in all of these conditions is small such that at these values they do not result in significant changes in the dimensions of the arm.

Table 4.13: Summary of Driveshaft Dynamic Analysis Results

Motor Torque	Maximum Equivalent Stress (MPa)	Maximum Deformation (mm)
Holding Torque (Angle Lock)	26.73	0.002
Full Torque (Variable Angle)	27.27	0.003
Maximum Motor Torque	31.64	0.007

4.9.5 Summary of Analysis

The analysis has shown the respective characteristics of both the arm and the shaft under various operating conditions. It is important for the shaft to have minimal deformation as it may result in the failure of the mechanism due to the clearance it needs to run through the hole in the arm. The arm must also maintain its shape for the same reason. With a combined maximum deformation of 0.032 for both the arm and the shaft at extreme operating condition, there is still a significant clearance distance between the hole diameter and shaft diameter. However, lubrication at this point or an excellent surface finish of these parts should be considered in fabrication to avoid unwanted friction. The analysis also shows that stress concentrations associated with the design is below the yield strength of the material and thus suggests the potential resistance of the mechanism against structural failure at normal operating conditions.

CHAPTER 5

CONCLUSION AND RECOMMENDATION

5.1 Conclusion

For this project, several UAV and VTOL concepts were studied in the conceptual design development and even the Harrier Jump Jet was studied to understand the principle behind the VTOL mechanism. Various power transfer devices and system drives were investigated for its suitability to be used in the design of the interlocking mechanism. Based on the data obtained from the reference projects the interlocking mechanism was designed to fulfill the necessary requirements especially in terms of geometric compatibility and spatial constraints.

The design selection process was done and the design was chosen based on several criteria considered to be important towards the design requirements. The design is simple and compact with a strong and rigid arm for support and a driveshaft to transfer the rotational motion to the fan. The parts are made of lightweight aluminum with simple fastening methods for ease of fabrication. The lightweight motor used is selected based on the spatial requirements of the mechanism complete with its own gearing system to address to the low revolution per minute requirement of the mechanism.

The 3-Dimensional graphical model of the mechanism was generated and analyzed to investigate its behavior under static and dynamic loading conditions. The assembled model can be broken down into the arm, motor and driveshaft while the arm and driveshaft was chosen to be analyzed. The analysis showed the stress and deformation of the parts under several operating conditions and it was then evaluated to identify the critical and possible points of failure. The analysis was completed with both parts showing good signs of resistance to stress and deformation and thus suggesting that the mechanism design is feasible and can be used for future development.

5.2 Recommendation

5.2.1 Control Mechanism

The project can be improved and enhanced by considering the use of control algorithm to included in future works. The mechanism has the ability to rotate the fans and thus gives an added degree of freedom for more advanced maneuver and control. With proper control and programming the variable angle capability of the fans can be utilized along with the quad rotor concept for better stability, performance and use of energy.

With the aid of a digital barometric sensor, the MUAV can measure altitude and thus it can be programmed to fly based on a specific flight plan for automated flight without the need for a remote pilot. This may also add to the stability of the MUAV and thus allowing for better indoor performance.

5.2.2 Further Analysis and Evaluation of Mechanism Design

The mechanism design should be further analyzed and evaluated to strengthen the credibility of the design concept. Vibration testing and fluid dynamics are some of the analysis that can be done to observe the effect of vibration on the mechanism as well as the effects of air drag on the mechanism performance. The use of Carbon-Carbon composites instead of aluminum should be considered as it could lead to further weight reduction.

5.2.3 Structural Improvement

The structural design of the MUAV needs to be further evaluated as there are issues regarding the flow of air at both limiting positions when the fans are rotated. There must be sufficient distance from the duct to the aircraft body to allow for a more effective air flow through the fans.

REFERENCES

- [1] Annibal Ollero & Luis Merino, *Control and Perception Techniques for Aerial Robotics*, 2004, Pablo de Olavide University, Sevilla, Spain
- [2] Sandin, P.E., *Robot Mechanisms and Mechanical Devices Illustrated*, 2003, USA, McGraw-Hill
- [3] Matt Ruff, *Servo Motor Control Application on a Local Interconnect Network*, 2005, Bit Division Systems Engineering, Austin, Texas
- [4] Brunigstrasse Sachseln, *Maxon Micro-drive*, Germany, November 2004 Edition
- [5] Robert Bosch, *Digital Pressure Sensor*, 2008, Germany, Doc. No.: BST-BMP085-DS000-03
- [6] Mohd Anuar Sulaiman, *Design of Micro Unmanned Aerial Vehicle Structure*, 2009, Unpublished Degree Dissertation, Universiti Teknologi Petronas, Malaysia
- [7] Wilfred Voss, *The Aspects of Servo Motor Sizing*, 2005, Copperhill Technologies Corporation
- [8] Vic Chen, *Motor Torque Calculation*, 2005, Leadshine Technology Co. Ltd.
- [9] Nor Hidayah Mohd Saini, *Design of Micro Unmanned Aerial Vehicle Vertical Takeoff and Landing Mechanism*, 2009, Unpublished Degree Dissertation, Universiti Teknologi Petronas, Malaysia
- [10] Tommaso Bresciani, *Modelling Identification and Control of a Quadrotor Helicopter*, 2008, Department of Automatic Control, Lund University

- [11] Charles E. Dole & James E. Lewis, *Flight Theory and Aerodynamics*, 2000, Wiley Interscience

- [12] Kaan T. Oner, Ertugrul Cetinsoy, Mustafa Unel, Mahmut F. Aksit, Ilyas Kandemir, Kayhan Gulez , *Dynamic Model and Control of a New Quadrotor Unmanned Aerial Vehicle with Tilt-Wing Mechanism*, 2008, World Academy of Science, Engineering and Technology, Volume 35

- [13] Frank Vann, *Harrier Jump Jet*, 1989, Brian Todd Publishing House Limited, USA

- [14] Ullman, D.G., 1997, *The Mechanical Design Process*, 2nd Edition, New York, McGraw-Hill

- [15] R.C. Hibbeler, 2007, *Engineering Mechanics Dynamics*, 11th Edition, Pearson Prentice Hall

- [16] Joseph E. Shingley & Charles R. Mischke, 2003, *Mechanical Engineering Design*, 6th Edition, New York, McGraw-Hill

- [17] Fitzer E, Manocha LM, 1998, *Carbon reinforcements and carbon-carbon composites*, Berlin, Springer-Verlag